Spin-exchange effects on tensor polarization of deuterium atoms

H. J. Bulten* and Z.-L. Zhou†
Department of Physics, University of Wisconsin, Madison, Wisconsin 53706

J. F. J. van den Brand
Department of Physics and Astronomy, Vrije Universiteit, 1081 HV Amsterdam, The Netherlands;
Nationaal Instituut voor Kernfysica en Hoge Energie Fysica (NIKHEF), 1009 DB Amsterdam, The Netherlands;
and Department of Physics, University of Wisconsin, Madison, Wisconsin 53706

M. Ferro-Luzzi
Nationaal Instituut voor Kernfysica en Hoge Energie Fysica (NIKHEF), 1009 DB Amsterdam, The Netherlands

J. Lang
Institut für Teilchenphysik, Eidgenössische Technische Hochschule, CH-8093 Zürich, Switzerland
(Received 16 October 1996; revised manuscript received 15 October 1997)

We present measurements of the effects of spin exchange on the nuclear tensor polarization of atomic deuterium gas. Measurements of the nuclear polarization have been performed at several values of the magnetic field. In these measurements, only the gas density was changed, leaving all other experimental parameters constant. The results are in qualitative agreement with a model, based on the spin-exchange mechanism proposed by Purcell and Field. The results are relevant for nuclear and particle-physics experiments, using nuclear polarized hydrogen or deuterium targets, as well as for laser optical pumping applications of ^{1}H and ^{2}H. [S1050-2947(98)03806-2]

PACS number(s): 34.50.−s, 39.10.+j, 29.25.Pj, 24.70.+s

I. INTRODUCTION

In nuclear and high-energy physics, the experimental study of spin-dependent observables is important for testing and constraining theoretical models. Spin-dependent scattering experiments provide information on, e.g., the spin structure functions of the nucleon, the electric form factor of the neutron, and the spin structure of few-body nuclei. For such experiments the availability of pure, nuclear-polarized hydrogen and deuterium targets is a great advantage. Recently, targets have been developed in which a nuclear-polarized atomic beam is injected into an open-ended T-shaped conductance limiter (hereafter referred to as storage cell) internal to a storage ring. In comparison to targets used at external beam facilities, these internal targets are characterized by high polarizations, rapid polarization reversal, high isotopic and chemical purity, flexible spin orientation, and small target thickness at high luminosity, allowing for high-precision experiments with small systematic errors. Experiments that make use of internal targets include the HERMES experiment at DESY [1], and experiments at BINP [2], NIKHEF [3], and IUCF [4–6].

The availability of intense, highly polarized internal targets was recently made possible by the development of coatings to prevent wall depolarization [7], the improvement in intensity of polarized atomic beams [8], and the development of precise polarimeters [9,10]. An essential issue is the influence of spin exchange between the atoms. Since the atomic density is increased by the use of storage cells to a level where atomic collisions occur with significant probability (>0.1), the effect of spin exchange on the polarization may be non-negligible and should be understood. Furthermore, the spin-exchange mechanism enables a novel way to produce polarized atoms [11], based on optical pumping of alkali metals. Here, the electron spin of hydrogen (or deuterium) is first polarized via spin-exchange collisions with the optically pumped alkali-metal atoms, and the *nuclear* spin is polarized via spin-exchange collisions between hydrogen (or deuterium) atoms. This development may lead to targets with significantly higher figure of merit, and it is vigorously pursued by different groups [12–14].

Measurements of spin exchange have been previously discussed in detail for alkali vapors (e.g., by Grossetête [15]). Here, we report on a measurement of the effects of the atomic density on the nuclear polarization for deuterium gas in a storage cell environment. Measurements of the nuclear tensor polarization were performed at different densities and external magnetic fields on tensor-polarized deuterium inside an electron storage ring. The results demonstrate a dependence of the nuclear polarization on the atomic density, which can be interpreted as caused by spin exchange.

In Sec. II we present a brief description of the spin-exchange mechanism and outline the theoretical background and formulas used in this work. Section III describes the experimental setup and the measurements. The results are summarized in Sec. IV.

*Present address: Department of Physics and Astronomy, Vrije Universiteit, 1081 HV Amsterdam, The Netherlands.

†Present address: Laboratory for Nuclear Science, Massachusetts Institute of Technology, Cambridge, MA 02139.

II. SPIN EXCHANGE RATE

The eigenvectors for ground-state deuterium atoms in an external magnetic field **B** are well known. The interaction Hamiltonian is given by

$$H=\frac{2h\nu_0}{3}\mathbf{I}\cdot J+\mu_B(g_I\mathbf{I}+g_J\mathbf{J})\cdot\mathbf{B} \tag{2.1}$$

in which **I** and **J** are the nuclear and electron spin, $g_I=-0.00047$ and $g_J=2.0023$ are the gyromagnetic factors, μ_B is the Bohr magneton and

$$h\nu_0=\mu_B(g_J-g_I)B_c$$

is the hyperfine splitting (ν_0 = 327 MHz). The critical field $B_c=11.7$ mT characterizes the average magnetic field due to the deuteron spin at the position of the electron. The spin part of the wave function for the six substates of atomic deuterium can be described as

$$|i\rangle=|m_I,m_J\rangle,$$

$$|1\rangle=|1,1/2\rangle,$$

$$|2\rangle=\alpha_{-+}|1,-1/2\rangle+\alpha_{++}|0,1/2\rangle,$$

$$|3\rangle=\alpha_{--}|0,-1/2\rangle+\alpha_{+-}|-1,1/2\rangle,$$

$$|4\rangle=|-1,-1/2\rangle,$$

$$|5\rangle=\alpha_{+-}|0,-1/2\rangle-\alpha_{--}|-1,1/2\rangle, \tag{2.2}$$

$$|6\rangle=\alpha_{++}|1,-1/2\rangle-\alpha_{-+}|0,1/2\rangle,$$

$$\alpha_{+\pm}=\sqrt{\frac{1}{2}(1+a_\pm)},$$

$$\alpha_{-\pm}=\sqrt{\frac{1}{2}(1-a_\pm)},$$

$$a_\pm=\left(x\pm\frac{1}{3}\right)\sqrt{1\pm\frac{2}{3}x+x^2},$$

$$x=B/B_c.$$

In Fig. 1 the tensor polarization P_{zz} ($P_{zz}=1-3n_0$, with n_0 the fraction of nuclei with $m_I=0$) is shown for each of these states. The dots on the curves indicate the magnetic field values that were applied in this experiment.

The collision of two atoms at thermal velocities can be described following Purcell and Field [16]. The large difference in energy for the molecular triplet and singlet states leads to a spin-flip probability of 50% for collisions between atoms with opposite electron spin. During the collision, the much weaker hyperfine interaction plays a negligible role. After the collision, the electrons and nuclei recombine into one of the six eigenstates under conservation of angular momentum. Especially at low field, where the coupling between nuclear and electron spin is important, a single atomic spin-exchange collision may lead to large changes in nuclear polarization.

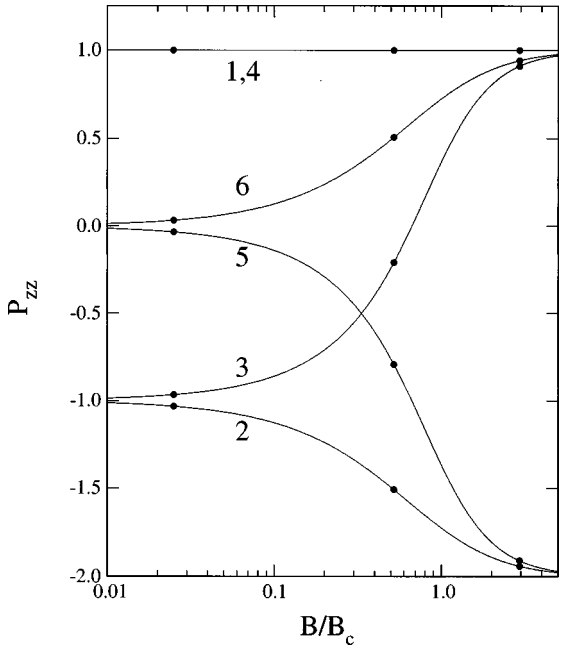

FIG. 1. Tensor polarization P_{zz} of the deuterium hyperfine states as a function of external field. The critical field B_c equals 11.7 mT.

The rate of spin exchange can be described by the rate equations [11]

$$\frac{d}{dt}n_i=\frac{1}{T_{dd}}\sum_{a,b}n_a n_b A^i_{a,b}(x), \tag{2.3}$$

where $1/T_{dd}=\rho_d\langle\sigma_{se}v\rangle$ is the spin-exchange collision rate, ρ_d represents the deuterium density, n_i the fractional density of atoms in state i, and $\langle\sigma_{se}v\rangle$ the average value for the product of the spin-exchange cross section and the velocity distribution. The value of $\langle\sigma_{se}\rangle$ was taken from Ref. [17]. The coefficients $A^i_{a,b}$ that describe the probability for states $|a\rangle$ and $|b\rangle$ to transform into state $|i\rangle$ are explicitly given by Ref. [18].

III. EXPERIMENT

A. Overview of the experimental setup

The measurements were performed with a tensor-polarized deuterium target internal to the AmPS electron ring at NIKHEF [19], in parallel with measurements of the tensor analyzing power T_{20} in (quasi) elastic electron scattering from deuterium [3]. Since the setup is extensively described in Refs. [9,20,21] here only a brief outline is given.

The experiment is outlined in Fig. 2. The electron beam had an energy of 704 MeV and currents of up to 100 mA. Nuclear-polarized deuterium gas was provided by an atomic beam source (ABS). This source [20,22] consists of an rf dissociator, a cooled nozzle, two sextupole electromagnets and two rf transition units [23]. The sextupole magnets focus, according to the Stern-Gerlach principle, atoms with electron spin up (states 1, 2, and 3) and reject the states with spin down (4, 5, and 6). Nuclear polarization is obtained by

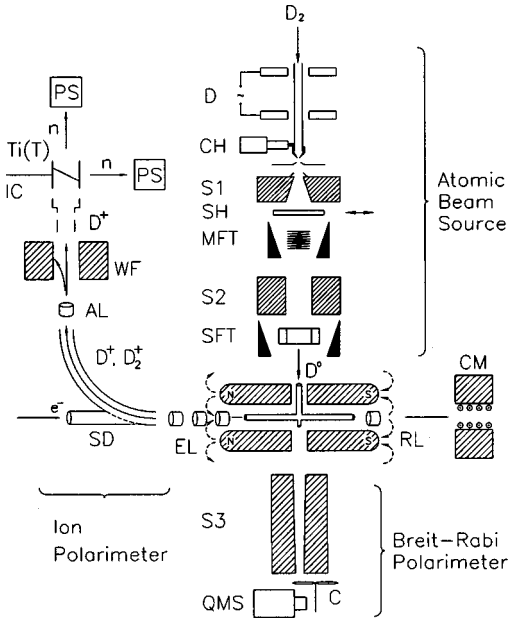

FIG. 2. Schematic outline of the atomic beam source, Breit-Rabi polarimeter, internal target, and ion-extraction polarimeter. All components, except the neutron detectors, the target holding field, and the correction magnets, are inside the vacuum system. *D*: RF dissociator; CH: cold head; *S*1, *S*2, *S*3: sextupole magnets; MFT, SFT: medium- and strong-field transition units; SH: shutter; *C*: chopper; QMS: quadrupole mass spectrometer; CM: correction magnet; RL: repeller lens; EL: triplet of ion-extraction lenses; SD: spherical electrostatic deflector; AL: electrostatic lens; WF: Wien filter; IC: ion collector; PS: neutron detector.

inducing rf transitions in the medium and/or strong field transition unit. The strong field unit induces either a 3-5 transition or a 2-6 transition. The medium field unit induces a 1-4 transition. Note that in this multiple-quantum transition the z projection of the angular momentum of the atom changes by $3\hbar$. The principle of operation of the 1-4 transition unit has been discussed by Oh [24]. The atomic beam from the ABS is injected into a storage cell. In this way the atomic density is increased by two orders of magnitude compared to that of a free atomic beam. The storage cell was cooled to about 150 K to further increase the target density and polarization. The cell has been constructed from ultrapure aluminum with a thickness of 25 μm. In order to minimize recombination and depolarization [7], it has been coated with a solution of PTFE3170 Teflon. The storage cell (feed tube) has a length of 400 mm (130 mm) and a diameter of 15 mm (12 mm). A small sample tube (4 mm diameter), located opposite to the feed tube, allows one to sample a fraction ($\sim$10%) of the injected gas, for subsequent analysis by a Breit-Rabi polarimeter.

This polarimeter consists of a 41-cm-long permanent tapered sextupole magnet [entrance (exit) radius 3 mm (1.5 mm), tip field about 0.44 T] in front of a quadrupole mass spectrometer. A chopper, located in between the magnet and the mass spectrometer, was employed to subtract background gas. The Breit-Rabi polarimeter was used to continuously monitor the performance of the ABS during data taking.

An external field, parallel to the electron beam, was supplied by two magnets that are located at opposite sides along the storage cell.

Nuclear polarization was measured *in situ* by a polarimeter [9], which uses the well-known tensor analyzing power [25] of the reaction $^3H(d,n)\alpha$. The electron beam ionizes a fraction of the deuterium gas in the storage cell. These ions are extracted by a set of electrostatic lenses and an electrostatic spherical deflector, accelerated to 60 keV and transported to a tritiated titanium target. The 14-MeV recoiling neutrons are detected in two neutron detectors, located under 0° and 90° with respect to the spin orientation axis. The angle-dependent count rate for the reaction $^3H(d,n)\alpha$ can be written as

$$N(\theta)=N_0\left(1-\frac{f}{4}P_{zz}[3\cos^2(\theta)-1]\right), \tag{3.1}$$

where θ is the angle between the neutron momentum and the polarization axis, $f=0.95$ for 60 keV deuterons [25], N_0 is the unpolarized count rate (typically 1 kHz), and P_{zz} the tensor polarization of the impinging deuterons. Separation of atomic (D^+) and molecular (D_2^+) ions was obtained by using a Wien filter.

With this polarimeter, the tensor polarization of the target could be measured to a statistical precision of 0.01 within about 1 min of beam time. The systematic uncertainty in the measurements can be greatly reduced by forming a ratio R [9], where

$$R=\sqrt{\frac{N^+(0°)N^-(90°)}{N^+(90°)N^-(0°)}} \tag{3.2}$$

in which N^+ (N^-) represents the rate with the highest (lowest) value of P_{zz}. In this ratio R, variations in luminosity and differences in detection efficiency cancel. The systematic error on P_{zz} measured with the tritium polarimeter is estimated to be 2%.

B. Measurements

The rate of spin exchange linearly depends on the atomic density and is a function of the external magnetic field [see Eq. (2.3)]. To isolate the effects of spin exchange on the tensor polarization we measured at two values of atomic density ($\rho_d=1.1\times10^{12}$ and 0.4×10^{12} atoms/cm^3).[1] Except for the number of atomic collisions, no other experimental parameters were changed. For the conditions of the present experiment, the average time between spin-exchange collisions T_{dd} was about 4.5 ms (12 ms) for measurements at the highest (lowest) density. The average dwell time in the cell was about 2.5 ms. The different densities were obtained by changing the flux of the ABS, which was done by adjusting the RF power of the discharge. Several measurements were made, activating either the medium field transition unit, the strong field transition unit, or both units. Sets of measurements with different densities were taken at three values of the external magnetic field (0.3, 6, and 34 mT).

[1]Note, that the use of a storage cell leads to an approximately triangular density distribution along the cell axis; the density quoted above refers to the center of the cell.

TABLE I. Hyperfine content of the injected atomic beam for the combinations of transitions, applied in the present experiment. The resulting value of P_{zz} is given for different values of external magnetic field.

Transition		Injected	P_{zz}		
MFT	SFT	states	0.3 mT	6.1 mT	34.4 mT
None	None	1,2,3	−0.333	−0.238	−0.010
1-4	None	2,3	−1.000	−0.857	−0.515
None	2-6	1,3,6	0.023	0.433	0.951
None	3-5	1,2,5	−0.023	−0.433	−0.951
1-4	2-6	3,6	−0.466	0.150	0.926
1-4	3-5	2,5	−0.167	−1.150	−1.926

In order to obtain small systematic errors, measurements were performed in the following way: for 4 s, the background rate of the neutron detectors (which is mainly due to interactions caused by the 704 MeV electron beam) was measured. This rate was obtained by changing the voltage of the spherical deflector plates such that no ions impinged on the tritium target. For the next three periods of 4 s, first no transition unit was activated (injecting states 1, 2, and 3), and then the medium field transition and the strong field 3-5 transition were induced, and finally the medium field transition and the strong field 2-6 transition were induced. This cycle of 16 s was repeated to obtain sufficient statistics and to verify the systematic stability of the polarimeter, i.e., that the measurements yield the same results within statistics upon repetition (with, e.g., new conditions of the electron beam). Note that the beam lifetime was around 1000 s so that the background rate varied slowly compared to our cycle period. Also other combinations of transitions were applied, e.g., cycles in which the medium field or strong field transition unit was switched off. Table I summarizes the hyperfine content of the injected atomic beam for the different applied transitions, and the corresponding value of tensor polarization P_{zz} for the magnetic fields at which the measurements were performed.

An example of the observed neutron rates during a polarization measurement is shown in Fig. 3. As can be seen, the background rate is about a factor of five lower than the signal from the $^3H(d,n)\alpha$ reaction. The background rate is rather stable in time and it is about equal for both detectors. (Note that during period II in this figure, three hyperfine states from the ABS are injected, while during periods III and IV only two states are injected.) The asymmetry is sizable, and the difference in tensor polarization (ΔP_{zz}) between the combinations of hyperfine states obtained with two different settings of the transition units can be determined quickly with high statistical precision.

We made measurements of (ΔP_{zz}) for combinations of the six settings of the RF transition units, listed in Table I. The presence of spin exchange is demonstrated in Fig. 4, which shows the average ratio of ΔP_{zz} for the measurements at high and at low density. Systematically, a higher value of ΔP_{zz} is found for the measurements at lower target density.

The calculations in Fig. 4 are based on the rate equations (2.3). For the spin exchange cross section, 2.3×10^{-15} cm^2 was taken [17]. The state density of the incoming deuterium

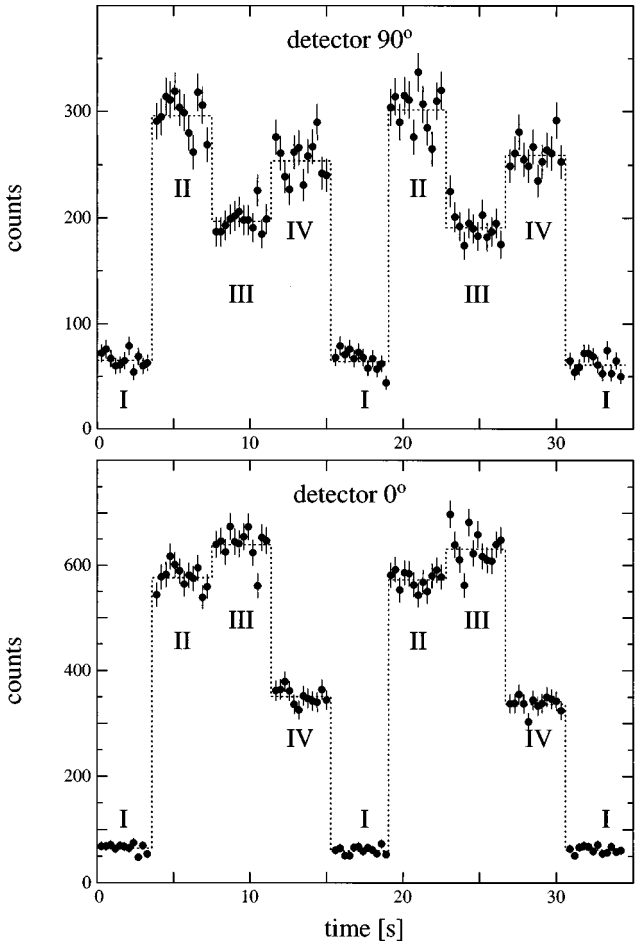

FIG. 3. Number of counts in 300-ms bins in the 90° (top) and 0° (bottom) neutron detector for the tritium polarimeter. Two measurement cycles are displayed. For this particular scan the background was measured in period I, whereas in period II, III, and IV the rates were measured with no transition units active, a SFT 3-5 and a MFT 1-4 transition, and a SFT 2-6 and a MFT 1-4 transition induced in the ABS, respectively.

atoms was calculated assuming 100% efficiency for the rf units in the ABS [20], but an 80% rejection efficiency for state 4 by the second sextupole magnet. In addition, we assumed that the incoming atomic beam was diluted with 26% of the unpolarized atoms to take into account a reduction of the polarization. This reduction of the polarization includes the following effects, which were not taken into account explicitly in our calculations: (1) depolarization of the atoms by collisions with the cell wall, (2) dissociative ionization of molecules (measured to contribute about 1%), (3) rejection efficiency of spin-down states by the first sextupole magnet in the ABS.

With these assumptions, the resulting polarization of the deuterium atoms in the target cell was calculated for the geometry and temperature of the present setup by numerically solving the rate equations. The actual density and magnetic field distributions along the storage cell and the feed tube were taken into account by a finite-element analysis: the cell (feed tube) was divided in 21 (10) segments. For each

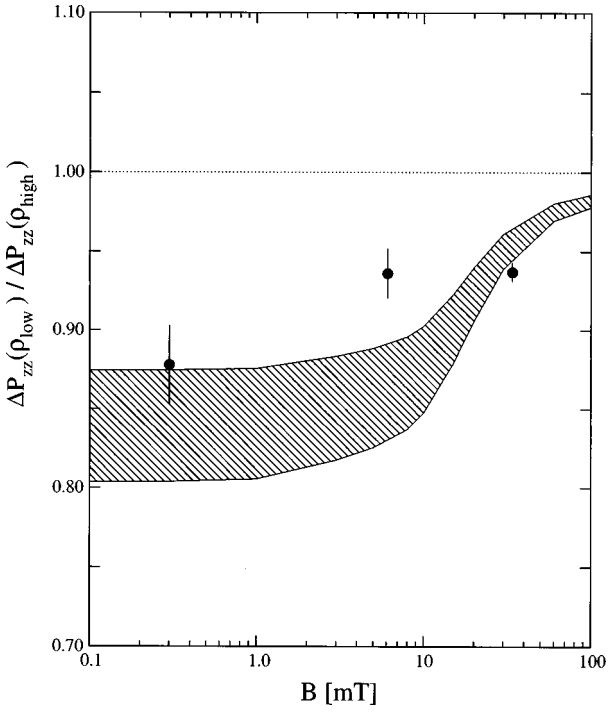

FIG. 4. Ratio of difference in tensor polarization ΔP_{zz} for measurements at high (1.1×10^{12} cm^{-3}) and low (0.4×10^{12} cm^{-3}) atomic density. The data show the average effect of different transitions. The hatched area represents the results of our model. The dotted line indicates the result in the absence of spin-exchange effects.

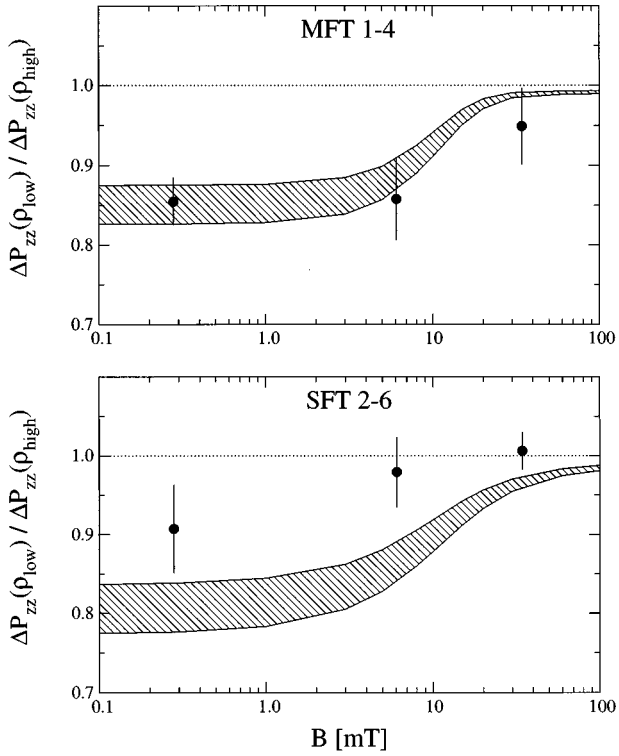

FIG. 5. Ratio of ΔP_{zz} for measurements at high (1.1×10^{12} cm^{-3}) and low (0.4×10^{12} cm^{-3}) atomic density for the 1-4 medium field transition (top) and the 2-6 strong field transition (bottom).

step in time (Δt is about 2 μs) the population density in each segment, as well as the amount of gas that flows to neighboring segments, was calculated. A sufficient number of steps in time was taken in order to assure that the final result was completely stable.

The results of our calculations are represented by the shaded band in Fig. 4. The width of this band indicates the uncertainty in the calculations, due to the uncertainty in the spin-exchange cross section [17] (10%) and the uncertainty in the target density in our measurements (20%). The results of the calculation for the different combinations of transitions in Fig. 4 were averaged in a similar manner as the data. Although the data show a smaller dependence on the external magnetic field than calculated by our model, qualitative agreement is obtained between the data and the model predictions.

The ratio of ΔP_{zz} for the different densities is explicitly shown in Fig. 5 for two transitions that give sizable tensor polarization for all external fields, i.e., the medium field 1-4 transition and the strong field 2-6 transition. For these transitions, the difference in tensor polarization ΔP_{zz} between injected states (1,2,3) and (2,3), respectively states (1,2,3) and (1,2,6), is measured. The calculations for the strong field transition (2-6) predict somewhat less reduction of the polarization, but the dependence on magnetic field is reproduced. The numerical results for the medium field transition (1-4) are in agreement with the data.

IV. SUMMARY

We measured the tensor polarization of a deuterium gas sample for different external magnetic fields (between 0.02 and 3.0 times the critical field) at two densities. The measurements demonstrate the effects of spin-exchange collisions between deuterium atoms. Changing the density of the deuterium gas, while keeping all other experimental parameters constant, resulted in differences in nuclear tensor polarization of typically 10%. The measurements indicate that spin exchange lowers the polarization in a storage cell by about 10% for densities of $\sim10^{12}$ atoms/cm^3, even for an external magnetic field that is three times larger than the critical field. The observed density-dependent reduction of the tensor polarization is in qualitative agreement with numerical calculations based on the model of Purcell and Field [16].

ACKNOWLEDGMENTS

We wish to express our gratitude to our colleagues of the 91-12 collaboration. This work was in part supported by National Science Foundation Grant. No. PHY-9316221, the Stichting voor Fundamenteel Onderzoek der Materie (FOM), which was financially supported by the Nederlandse organisatie voor Wetenschappelijk Onderzoek (NWO), and the Swiss National Foundation.

[1] HERMES experiment at DESY, DESY Report No. DESY-PRC 93-06, 1993 (unpublished).
[2] V. F. Dmitriev *et al.*, Phys. Lett. **157B**, 143 (1985); B. B. Voitsekhovskii *et al.*, JETP Lett. **43**, 733 (1985); R. Gilman *et al.*, Phys. Rev. Lett. **65**, 1733 (1990).
[3] M. Ferro-Luzzi *et al.*, Phys. Rev. Lett. **77**, 2730 (1996).
[4] IUCF experiment CE-35; see W. Haeberli, in *Proceedings of the 8th International Symposium on Polarization Phenomena in Nuclear Physics,* edited by E. J. Stephenson and S. E. Vigdor, AIP Conf. Proc. No. 339 (AIP, New York, 1994), p. 213.
[5] K. Lee *et al.*, Phys. Rev. Lett. **70**, 738 (1993).
[6] M. A. Miller *et al.*, Phys. Rev. Lett. **74**, 502 (1995).
[7] J. S. Price and W. Haeberli, Nucl. Instrum. Methods Phys. Res. A **349**, 321 (1994).
[8] T. Wise, A. D. Roberts, and W. Haeberli, Nucl. Instrum. Methods Phys. Res. A **336**, 410 (1993); F. Stock *et al.*, Nucl. Instrum. Methods Phys. Res. A **343**, 334 (1994).
[9] Z.-L. Zhou *et al.*, Nucl. Instrum. Methods Phys. Res. A **379**, 212 (1996).
[10] H.-G. Gaul and E. Steffens, Nucl. Instrum. Methods Phys. Res. A **316**, 297 (1992).
[11] T. Walker and L. W. Anderson, Nucl. Instrum. Methods Phys. Res. A **334**, 313 (1993).
[12] K. Coulter *et al.*, Phys. Rev. Lett. **68**, 174 (1992); M. Poelker *et al.*, Phys. Rev. A **50**, 250 (1994).
[13] J. Stenger, Ph.D. thesis, Friedrich Alexander Universität Erlangen-Nürnberg, Germany, 1995 (unpublished).
[14] H. Gao, R. Cadman, R. J. Holt, and E. Thorsland, in *Proceedings of the International Workshop on Polarized Beams and Polarized Gas Targets,* edited by H. Paetz gen. Schiek and L. Sydow (World Scientific, Singapore, 1995), p. 67.
[15] F. Grossetête, J. Phys. (Paris) **29**, 456 (1968).
[16] E. M. Purcell and G. B. Field, Astrophys. J. **124**, 542 (1956).
[17] M. Desaintfuscien and C. Audoin, Phys. Rev. A **13**, 2070 (1976); A. C. Allison, *ibid.* **5**, 2695 (1972).
[18] J. Stenger and K. Rith, Nucl. Instrum. Methods Phys. Res. A **361**, 60 (1995); **378**, 360 (1996).
[19] G. Luijckx *et al.* (unpublished).
[20] Z.-L. Zhou *et al.*, Nucl. Instrum. Methods Phys. Res. A **378**, 40 (1996).
[21] E. Passchier *et al.*, Nucl. Instrum. Methods Phys. Res. A **387**, 471 (1997).
[22] D. Singy, W. Grüebler, P. A. Schmelzbach, O. Huwyler, and W. Z. Zhang, Nucl. Instrum. Methods Phys. Res. A **306**, 36 (1991).
[23] M. Ferro-Luzzi, Z.-L. Zhou, H. J. Bulten, and J. F. J. van den Brand, Nucl. Instrum. Methods Phys. Res. A **364**, 44 (1995).
[24] S. Oh, Nucl. Instrum. Methods **82**, 189 (1970).
[25] G. G. Ohlsen, J. L. McKibben, and G. P. Lawrence (unpublished).